Electronic Energy Transfer in Multichromophoric Arrays. The Effects of Disorder on Superexchange Coupling and Energy Transfer Rate

Edwin K. L. Yeow and Kenneth P. Ghiggino*

Photophysics Laboratory, School of Chemistry, The University of Melbourne, Parkville, Victoria 3052, Australia

Received: November 30, 1999; In Final Form: March 28, 2000

The effects of diagonal (site energy) and off-diagonal (intermolecular interaction) disorder arising from the distribution of ionization energies on superexchange coupling and the corresponding electronic energy transfer (EET) rate are considered. The effective donor−acceptor coupling is obtained using the Dyson's equations-based solution of the Green's function for both the orthogonal and nonorthogonal basis sets. In a disordered multichromophoric array, the effective superexchange coupling is shown to be enhanced. Furthermore, the competing roles of the multiple pathways when next-to-nearest-neighbor interactions exist behave differently depending on the type and extent of disorder. It is demonstrated that the exponential falloff of the energy transfer rate with increasing donor−acceptor distance weakens when disorder is present. Moreover, this exponential decay is more apparent when the donor−bridge energy gap is reduced. A method to treat EET at the molecular orbital level using Dyson's equations is also presented when the coupling between adjacent bridge sites is either Dexter or through-configuration interaction. We find that the superexchange coupling derived from the through-configuration interaction is the dominant mode of superexchange EET. The implications of the results for the design of molecular arrays with optimized energy transfer properties are considered.

1. Introduction

Both experimental and theoretical studies have recently been devoted to the elucidation of the mechanisms responsible for electronic energy transfer (EET) from an initially excited donor chromophore to an acceptor chromophore.[1−4] Such investigations are of crucial importance to the understanding of energy transfer dynamics in biological systems such as the photosynthetic unit, and in synthetic light harvesting systems.[4] A key objective is to equip photochemists with the required knowledge to design optimized structures for application in photomolecular devices.

Bridge-mediated or superexchange energy transfer has been proposed to be important in photosynthetic systems whereby intervening protein molecules are capable of mediating electronic coupling between the localized donor (D) and acceptor (A) molecules. It is now established that when through-space coupling is negligible between D and A, the excitation energy is still able to tunnel across the bridge states to the acceptor chromophore.[5] An example was given in paper 1 in this series[1a] where it was concluded that through-bond interaction is the dominant mechanism in the EET dynamics for a rigidly linked naphthalene dimer with the chromophores separated by six sigma bonds. This rate is nonadiabatic and is given by the classic Fermi's golden rule expression

$$k = \frac{2\pi}{\hbar}|H_{DA}|^2\delta(E_D - E_A) \tag{1}$$

where H_{DA} is the bridge mediated electronic coupling and the Dirac delta term ensures energy conservation between the two states.

The most common analytical expression used to describe this indirect coupling is the McConnell model[6]

$$H_{DA} = \left(\frac{V^2}{\omega}\right)\left(\frac{v}{\omega}\right)^{m-1} \tag{2}$$

where V is the coupling of A and D to the bridge, v is the coupling between the bridge components, ω is the excitation energy difference between the donor/acceptor and the bridge, and m is the number of bridge units. Equation 2 predicts an exponential decay of the magnitude of H_{DA} with increasing bridge length. The superexchange interaction results primarily from the short-range orbital-overlap dependent interaction between the constituent molecules. The effective overlap between the wave functions of the donor and acceptor thus arises from the mixing of these wave functions with the bridge orbitals. Several electronic factors such as Dexter's exchange integral, penetration terms, and through-configuration interaction have been proposed to promote such mixing.[7] The commonly invoked Dexter's theory and the through-configuration interaction have recently been examined closely.[7] We shall study the roles of both mechanisms here using a different approach.

The McConnell model suffers from approximations which can be removed when the Green's function formalism is used to treat superexchange coupling. Evenson and Karplus[8] have managed to use the partitioning technique to evaluate a closed form expression for H_{DA} which reduces to the McConnell's equation in the limit of $|\omega| \gg |2v|$. The Green's function method has been extensively used in the problem of electron transfer.[8−12] Of great interest to us is the solution of the Green's function elements via the Dyson's equations, first introduced by da Gama[12] to obtain the superexchange electron transfer rate. As demonstrated by da Gama and others,[13,14] this powerful

* Corresponding author. E-mail: k.ghiggino@chemistry.unimelb.edu.au.

10.1021/jp994218n CCC: $19.00
Published on Web 05/26/2000

technique eliminates the need to perform tedious matrix inversion and leads naturally to the tunneling pathway method.

When energy transfer measurements are conducted in the condensed phase, disorder in the form of diagonal site energy and off-diagonal intersite coupling fluctuations may occur.[15] The former corresponds to a fluctuation of transition frequencies of the individual molecules due to different molecular environments, while the latter implies a variation of the intermolecular interaction brought about by physical irregularity (e.g., positional disorder) of the molecular chain itself. It will be shown in this work that both diagonal and off-diagonal disorders can result from a perturbation of the ionization potential energies. Such heterogeneity has been known to affect the optical properties of polymers,[16] molecular aggregates,[17] and even photosynthetic systems.[18,19] In particular, through-space energy transfer rates and lifetimes are affected in disordered systems.[20,21] On the other hand, the effects of disorder on the superexchange coupling involved in EET have attracted little attention. Studies in this area have usually considered electron transfer.[22−24] In this paper, we shall emphasize superexchange EET and show the nexus between energy transfer and electron transfer.

We shall employ the Dyson's equations-based solution to the Green's function to demonstrate the behavior of the superexchange energy transfer rate in the presence of disorder. One-dimensional chain systems with only nearest-neighbor (NN) interactions are first considered. This is then extended to a system where next-to-nearest-neighbor (NNN) interactions exist. Such interactions give rise to multiple pathways for the transfer of excitation energy between donor and acceptor.[1c] Constructive and destructive interferences between different routes are possible and the effects of disorder on the competing roles of these pathways will be investigated.

An inspiration for this paper is also derived from the continuous effort to offer plausible explanations for the unprecedented ultrafast energy transfer rates observed in real molecular systems studied in this laboratory. Such anomalous rapid energy transfer is evident in dimethoxynaphthalene−norbornane bridge-ketone molecules[25] and the complex poly(acenaphthalene) polymers.[1b,26] In these systems, through-space coupling between the donor and acceptor chromophores is unable to completely explain the energy transfer mechanism. Through-bond interaction, on the other hand, is subject to the distance attenuation factor. This leads to another purpose of this paper, namely an investigation of the dependence of the attenuation factor on varying amounts of disorder. Working with real systems involves the nonorthogonality of the orbital basis which will be included in our Dyson's equations.

Several questions pertaining to the superexchange coupling and the corresponding energy transfer rate can therefore arise when disorder effects are considered.

1. What are the effects of diagonal and off-diagonal disorder? How would increasing the disorder affect the transfer rate?

2. What is observed when disorder is introduced into a system where NNN interaction exists? In particular, how would the effective donor−acceptor coupling contributions of individual pathways be affected?

3. Through-medium energy transfer is known to fall off exponentially with increasing donor−acceptor separation with a decay rate of β. Would β change with disorder?

4. How would the superexchange coupling change when either Dexter interaction or through-configuration interaction is used to describe adjacent bridge interaction?

These issues will be addressed in this paper which is organized as follows. In section 2, the Dyson's equations-based Green's function method is introduced and applied to the orthogonal and nonorthogonal basis systems. Methods for calculating Dexter's and through-configuration interaction are developed at the molecular orbital level. The Monte Carlo computational results are presented in section 3 along with the discussion. Finally, section 4 summarizes the results and implications of this work, and discusses possible experimental applications.

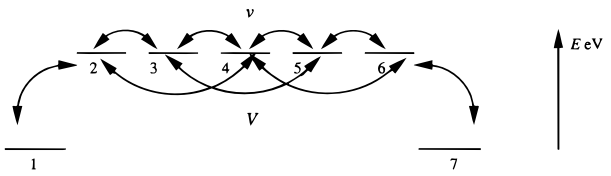

Figure 1. Schematic energy level diagram for a one-dimensional chain consisting of a donor (site 1) and an acceptor (site 7) connected via a five bridge sites system (sites 2, 3, 4, 5, and 6). The nearest-neighbor interaction (NN) is denoted by v_i while the next-to-nearest-neighbor interaction (NNN) between bridge units is denoted by V_j.

2. Theory and Method

(a) Orthogonal Basis. We consider a one-excitation Hamiltonian for our system

$$H = \sum_n \epsilon_n |n\rangle\langle n| + \sum_{n,m} \sum_{n\neq m} V_{n,m} |n\rangle\langle m| \tag{3a}$$

$$= \sum_{n,m} H_{n,m} |n\rangle\langle m| \tag{3b}$$

Here the $|n\rangle$ represents the state in which molecule n ($n = 1, 2, ..., N$) is excited and all other molecules are in their ground state. ϵ_n is the energy of the excited molecule n and $V_{n,m}$ describes the intermolecular interaction between molecules n and m. Direct through-space coupling between the donor and acceptor will be ignored throughout this work.

The Green's function elements for the above Hamiltonian can be easily obtained from the Dyson's equations. Equation 4 gives the Dyson's equations when orthogonal basis is considered[12]

$$EG_{i,j} = \delta_{ij} + \sum_k H_{i,k} G_{k,j} \tag{4}$$

and E is the tunneling energy for the excitation. For the case of only nearest-neighbor (NN) interactions between the molecules, the set of Dyson's equations for our model system consisting of a donor (site 1) and an acceptor (site 7) connected by 5 bridges (sites 2, 3, ..., 6) (see Figure 1) is given as

$$\begin{aligned}
(E-\epsilon_1)G_{11} &= 1 + H_{12}G_{21} \\
(E-\epsilon_2)G_{21} &= H_{21}G_{11} + H_{23}G_{31} \\
(E-\epsilon_3)G_{31} &= H_{32}G_{21} + G_{34}G_{41} \\
(E-\epsilon_4)G_{41} &= H_{43}G_{31} + H_{45}G_{51} \\
(E-\epsilon_5)G_{51} &= H_{54}G_{41} + H_{56}G_{61} \\
(E-\epsilon_6)G_{61} &= H_{65}G_{51} + H_{67}G_{71} \\
(E-\epsilon_7)G_{71} &= H_{76}
\end{aligned} \tag{5}$$

Stepwise renormalization of the above equations reduces all information onto the single site 1 (the donor)

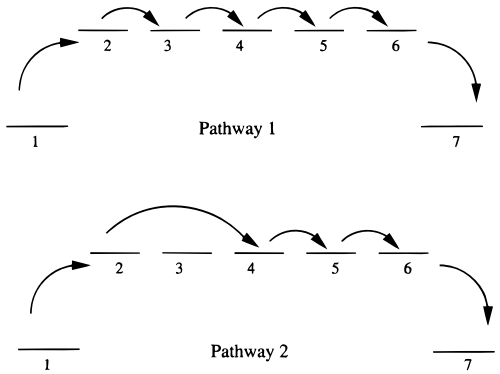

Figure 2. Schematic depiction of two possible pathways taken for the transfer of excitation energy from the donor to the acceptor. (a) and (b) represent pathway 1 and pathway 2, respectively, as discussed in the text.

$$(E - \epsilon_1 - \Delta_1)G_{11} = 1 + H_{17}G_{71} \tag{6}$$

The effective superexchange coupling between the donor and acceptor is thus given by

$$H_{17} = \left[\prod_{i=1}^{5} \frac{H_{i,i+1}}{(E - \epsilon_{i+1} - \Delta_{i+1})}\right] H_{67} \tag{7}$$

where

$$\Delta_i = \frac{H_{i,i+1}H_{i+1,i}}{E - \epsilon_{i+1} - \Delta_{i+1}} \tag{8}$$

Δ_i is defined to be the self-energy part of site i and accounts for all the information on the sites removed during the renormalization procedure. An obvious advantage of the coupling form given in eq 7 is that the through-medium coupling attenuation between sites i and i+1 is conveniently given by

$$t_i = \frac{H_{i,i+1}}{E - \epsilon_{i+1} - \Delta_{i+1}} \tag{9}$$

When next-to-nearest-neighbor (NNN) interactions (V_1, V_2, and V_3 of Figure 1) between the bridge sites are included, the whole system can again be reduced to the donor site using the renormalization method. In this case, different pathway contributions to the effective superexchange coupling can be achieved. In particular, a five-bridge system gives rise to 43 different possible pathways of which only two of them will be examined here (Figure 2). The route which includes only nearest-neighbor interactions (1 → 2 → 3 → 4 → 5 → 6 → 7) is chosen to be pathway 1 whereas pathway 2 has a NNN subroute replacing two NN subroutes (1 → 2 → 4 → 5 → 6 → 7). Pathway 2 is said to be an order smaller than pathway 1 since the number of sites visited is one smaller (i.e., site 3 is not encountered in pathway 2). Both pathways are ideal to investigate as their total path lengths are reasonably short and hence are vital routes taken by the excitation to go from donor to acceptor. Furthermore, the pathways' contributions to the effective superexchange coupling are of opposite sign, resulting in destructive interference effects. The superexchange coupling contributions for each pathway are given by

$$H_{17}^{\text{pathway1}} = \left[\prod_{i=1}^{5} \frac{H_{i,i+1}}{(E - \epsilon_{i+1} - \Delta_{i+1})}\right] H_{67} \quad \text{(pathway 1)} \tag{10}$$

$$H_{17}^{\text{pathway2}} = \frac{H_{12}H_{24}H_{45}H_{56}H_{67}}{(E - \epsilon_2 - \Delta_2)(E - \epsilon_4 - \Delta_4)(E - \epsilon_5 - \Delta_5)(E - \epsilon_6)} \quad \text{(pathway 2)} \tag{11}$$

Because of the NNN interactions, the site-energy parts in eqs 10 and 11 are different from eq 8. An example is given below

$$\Delta_4 = \frac{H_{46}H_{64}}{(E - \epsilon_6)} + \frac{H_{45}H_{54}}{(E - \epsilon_5 - \Delta_5)} + \frac{H_{45}H_{56}H_{64}}{(E - \epsilon_6)(E - \epsilon_5 - \Delta_5)} + \frac{H_{46}H_{65}H_{54}}{(E - \epsilon_6)(E - \epsilon_5 - \Delta_5)} + \frac{H_{46}H_{65}H_{56}H_{64}}{(E - \epsilon_6)^2(E - \epsilon_5 - \Delta_5)} \tag{12a}$$

where

$$\Delta_5 = \frac{H_{56}H_{65}}{E - \epsilon_6} \tag{12b}$$

(b) Nonorthogonal Basis. Analogous to electron transfer (ET), the Green's function method using Dyson's equations can be used to treat electronic energy transfer at the molecular orbital level. Appropriate treatment and inclusion of orbital overlap integrals for nonorthogonal basis states must be considered when formulating the superexchange coupling term. It will be shown here that the main difference between EET and ET is the involvement of two orbital overlap integrals in the former. This would therefore necessitate a more complex approach to correctly describe the superexchange rate in EET.

Until quite recently, many workers have been relying on the classical Dexter interaction to interpret EET kinetics between chromophores which are in close proximity. This has been shown by Harcourt et al.[7] to be an erroneous description of the energy transfer dynamics. In their analysis, the need to consider the interactions between ionic charge transfer configurations and locally excited states was advanced. This results in through-configuration interaction between donor and acceptor molecules. The contribution from the Dexter exchange integral is canceled out during the derivation of the through-configuration interaction term when the Mulliken approximation is employed.[7] It is therefore worth investigating how the superexchange coupling is affected by considering each mechanism and the effects of disorder. We begin by first deriving the superexchange coupling when only Dexter interaction occurs between adjacent bridge sites before proceeding on with the through-configuration interaction.

We define (a,a') and (b,b') to be the (HOMO,LUMO) of molecules A and B, respectively. The Dexter-type exchange integral contribution to the overall electronic coupling between A and B separated by a distance of r_{AB} is given by[27]

$$H_{AB}^{\text{Dexter}} = -\left\langle a'b\left|\frac{1}{r_{AB}}\right|b'a\right\rangle \tag{13a}$$

$$= -(a'b'|ba) \tag{13b}$$

Using the Mulliken approximation[28]

$$H_{AB}^{\text{Dexter}} = -\frac{1}{4}S_{ab}S_{a'b'}[(a'a'|bb) + (a'a'|aa) + (b'b'|bb) + (b'b'|aa)] \tag{14}$$

where $(a'a'|bb)$ is the Coulomb repulsion between electrons on $a'a'$ and bb and s_{ab} ($s_{a'b'}$) is the overlap integral of orbitals a (a') and b (b') (i.e., $s_{ab} = \langle a|b\rangle$). We can approximate the one-center integral by

$$(a'a'|aa) = (I_a + I_{a'})/2 \tag{15}$$

$$(b'b'|bb) = (I_b + I_{b'})/2 \tag{16}$$

where I_i is the ionization potential of orbital i. Electron affinity terms are taken to be zero for ease of analysis without affecting the overall conclusions. The two-center integral is approximated via the Mataga−Nishimoto formula[29] such that

$$(a'a'|bb) = \frac{e^2}{r_{AB} + \dfrac{2e^2}{I_{a'} + I_b}} \tag{17}$$

H_{AB}^{Dexter} is thus given by eq 18

$$H_{AB}^{Dexter} = -\frac{1}{4}s_{ab}s_{a'b'}\left[\frac{e^2}{r_{AB} + \dfrac{2e^2}{I_{a'} + I_b}} + \frac{e^2}{r_{AB} + \dfrac{2e^2}{I_a + I_{b'}}} + \frac{1}{2}(I_a + I_{a'} + I_b + I_{b'})\right] \tag{18}$$

As espoused by Harcourt et al.,[7] the Dexter term may not be the dominant electronic factor in the "short-range" orbital-dependent coupling. Instead, at close proximity, it was found that the more important factor is the through-configuration interaction term arising from the mixing between the locally excited and ionic configuration states. In this case[7]

$$H_{AB}^{tc} = \frac{2\beta_{ab}\beta_{a'b'}}{\bar{A}} \tag{19}$$

where $\bar{A}$ is the energy gap between the locally excited state and the charge transfer state. The bond integrals β_{ab} and $\beta_{a'b'}$ are given in eqs 20

$$\beta_{ab} = h_{ab} - s_{ab}h_{aa} \tag{20a}$$

$$\beta_{a'b'} = h_{a'b'} - s_{a'b'}h_{a'a'} \tag{20b}$$

h_{ii} is taken as $-I_i$ from Koopmans' Theorem[30] and h_{ij} is approximated using the Wolfsberg−Helmholz formula:[31]

$$h_{ij} = 0.5K(h_{ii} + h_{jj})s_{ij} \tag{21}$$

The Huckel constant K assumes a value of 1.75 in this work. Equation 21 is the usual formula used to compute the off-diagonal Hamiltonian elements in electron transfer. It is clear from eqs 18 and 19−21 that two overlap integrals (s_{ab}, $s_{a'b'}$) are necessary to effectively describe energy transfer hence distinguishing EET from ET.

Using Löwdin's partitioning method,[32] we arrive, for a nonorthogonal basis at the interaction term for the coupling between the donor (site 1) and the acceptor (site N) connected via $N - 1$ bridges (sites 2, 3, ..., $N - 1$)[33]

$$H_{1,N} = (H_{12} - ES_{12})G_{2,N-1}(H_{N-1,N} - ES_{N-1,N}) \tag{22}$$

The Green's function elements for the bridge system can be derived from Dyson's equations

$$\sum_l G_{il}(ES_{lj} - H_{lj}) = \delta_{ij} \tag{23}$$

such that for a model system with five bridge units, G_{26} is given by

$$G_{26} = \{(ES_{23} - H_{23})(ES_{34} - H_{34})(ES_{45} - H_{45})(ES_{56} - H_{56})\}/\{\hat{\alpha} - \hat{\beta}\hat{\gamma}\} \tag{24}$$

where

$$\hat{\alpha} = -[(ES_{54} - H_{54})(ES_{45} - H_{45})(ES_{66} - H_{66})][-(ES_{32} - H_{32})(ES_{23} - H_{23}) + (ES_{22} - H_{22})(ES_{33} - H_{33})] \tag{25a}$$

$$\hat{\beta} = (ES_{22} - H_{22})(ES_{43} - \dot{H}_{43})(ES_{34} - H_{34}) - \{(ES_{44} - H_{44})[-(ES_{32} - H_{32})(ES_{23} - H_{23}) + (ES_{22} - H_{22})(ES_{33} - H_{33})]\} \tag{25b}$$

$$\hat{\gamma} = [-(ES_{65} - H_{65})(ES_{56} - H_{56}) + (ES_{55} - H_{55})(ES_{66} - H_{66})] \tag{25c}$$

Now

$$ES_{ii} - H_{ii} = H_{11}S_{ii} - H_{ii} = \mathrm{EX}(1)S_{ii} - \mathrm{EX}(i) \tag{26}$$

where EX(i) is the excitation energy of molecule i and $S_{ii} = 1$. Since the tunneling energy cannot assume the unreasonably large value of the locally excited configuration energy H_{11}, which increases rapidly with the number of bridges, E is naturally chosen to be EX(1). The configuration overlap integral is obtained via[7]

$$S_{AB} = \begin{cases} -s_{ab}s_{a'b'} & A \neq B,\ |A - B| = 1 \\ 0 & A \neq B,\ |A - B| \neq 1 \\ 1 & A = B \end{cases} \tag{27}$$

Similar expressions can also be derived for different bridge lengths.

(c) Disorder and Computation Method. We assume a Gaussian disorder distribution $F(x)$ with standard deviation D for both the offset bridge energies ϵ_i (diagonal disorder) and the bridge−bridge couplings v_i (off-diagonal disorder) in the case of the orthogonal basis system

$$F(x) = \frac{1}{D\sqrt{2\pi}}\exp\left[-\frac{1}{2}\left(\frac{x - \mu}{D}\right)^2\right] \tag{28}$$

D varies from 0 to 0.4 eV (3226 cm^{-1}) for diagonal fluctuation and 0 to 0.1 eV (806 cm^{-1}) for off-diagonal fluctuation. This assumption has been successfully used in studies of aggregates[15] and photosynthetic light harvesting systems[34] where uncorrelated fluctuations are induced.

Disorder is added into the nonorthogonal basis system via the ionization potential energies, I_i. Using Koopmans' theorem, we can write the singlet transition energy for an excited molecule as[35]

$$\mathrm{EX} = I_\alpha - I_{\alpha'} + T \tag{29}$$

where α and α' are the HOMO and LUMO of the chromophore and T consists of Coulombic and exchange integrals. If disorder causes EX to be normally distributed with a Gaussian density function, then I_α and $I_{\alpha'}$ can also be assumed to be displaced

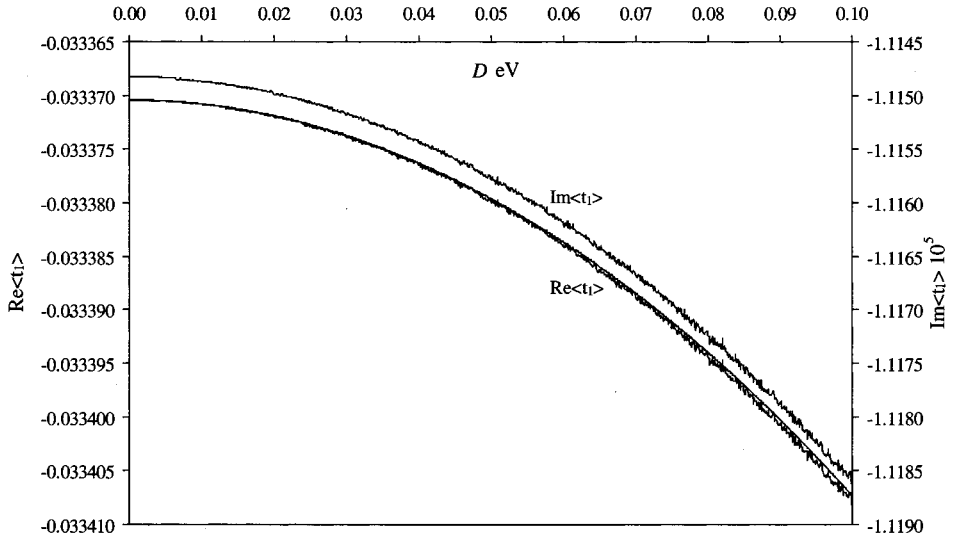

Figure 3. The effects of disorder on the real ($\mathrm{Re}\langle t_1\rangle$) and imaginary ($\mathrm{Im}\langle t_1\rangle$) components of $\langle t_1\rangle$. The analytical $\mathrm{Re}\langle t_1\rangle$ obtained from eqs 35 and 36 is given as the solid line.

according to eq 28. It is important to note that using the approach introduced here (see eqs 19−21) off-diagonal disorder can arise from a distribution of ionization potential energies and a probability distribution of interchromophoric distances. The latter significantly affects the orbital overlap integrals. In section 3b, off-diagonal disorder is solely induced from a distribution of ionization potential energies, while keeping the interchromophoric distances, and hence the orbital overlap integrals fixed.

Monte Carlo simulations were performed on ensembles of linear chains. All relevant parameters were obtained by averaging over 100 000 chains, and the inverse transform method[36] was employed to generate random variables with a Gaussian probability distribution. Computations were all carried out on a Cray J916 computer.

3. Results and Discussion

(a) Orthogonal Basis. We start our discussion by first examining the tunneling excitation energy E which can be obtained by repeated diagonalization of the Schrödinger equation in the partitioning method.[33] Often it is just assumed to be the effective donor and acceptor term without including any vibronic states or vibronic coupling effects. This is an incomplete description of the tunneling energy since EET proceeds between the continua, rather than single, vibronic states of the donor and acceptor chromophores.[1c] To correct for this neglect, a small complex parameter $i\tilde{\kappa}$ ($= 0.001i$) is introduced such that the tunneling energy becomes[37,38]

$$E = \epsilon_1 + i\tilde{\kappa} \tag{30}$$

Though this treatment is phenomenological in nature and lacks rigorous finesse, it has been shown in previous works that it is usually adequate to avoid undue divergences in the resonance region.[11,38]

To illustrate the effects of diagonal and off-diagonal disorder on the rate of superexchange energy transfer, a simple system consisting of chemically similar donor and acceptor chromophores with donor−bridge energy gap of 3 eV (24 195 cm^{-1}) is considered. Interchromophoric interactions are assumed to be 0.1 eV (806 cm^{-1}) throughout the chain and $\epsilon_1 = 2$ eV. An insight into the behavior of the superexchange coupling with disorder can be obtained by first examining the coupling attenuation factor between sites i and $i + 1$, t_i. Say, when $i = 1$, eq 9 can be rewritten for the average of t_1 over disorder

$$\langle t_1\rangle = \left\langle \frac{H_{12}}{E - \epsilon_2 - \Delta_2} \right\rangle \tag{31}$$

The spectrum for the real ($\mathrm{Re}\langle t_1\rangle$) and imaginary ($\mathrm{Im}\langle t_1\rangle$) parts of $\langle t_1\rangle$ are presented in Figure 3. Disorder is present in the form of fluctuation of the coupling between bridges 2 and 3, v_2. It is shown that the absolute magnitudes of $\mathrm{Re}\langle t_1\rangle$ and $\mathrm{Im}\langle t_1\rangle$ increase with disorder and the primary factor of $\langle t_1\rangle$ is the real component.

The above observation can be further appreciated by deriving the analytical expression for $\mathrm{Re}\langle t_1\rangle$. We can rewrite eq 31 to give

$$\langle t_1\rangle = \left\langle \frac{v_1(\epsilon_1 - \epsilon_3)}{(E - \epsilon_2)(\epsilon_1 - \epsilon_3) - v_2^2} \right\rangle \tag{32}$$

where the simplified form of Δ_2 is used

$$\Delta_2 = \frac{v_2^2}{\epsilon_1 - \epsilon_3} \tag{33}$$

This simplification is valid because all other omitted terms (e.g., Δ_3) in Δ_2 are relatively insignificant. $\mathrm{Re}\langle t_1\rangle$ is therefore given by

$$\mathrm{Re}\langle t_1\rangle = \left\langle \frac{v_1(\epsilon_1 - \epsilon_3)[(\epsilon_1 - \epsilon_2)(\epsilon_1 - \epsilon_3) - v_2^2]}{[(\epsilon_1 - \epsilon_2)(\epsilon_1 - \epsilon_3) - v_2^2]^2\,[\tilde{\kappa}(\epsilon_1 - \epsilon_3)]^2} \right\rangle \tag{34}$$

Using the virtual-crystal approximation[39] where self-averaging is assumed, the value obtained from any configuration is similar to the ensemble averaged value over all possible configurations. Since our sample size is reasonably large, the above assumption holds. In this case, eq 34 is recast into

$$\mathrm{Re}\langle t_1\rangle = \{v_1(\epsilon_1 - \epsilon_3)[(\epsilon_1 - \epsilon_2)(\epsilon_1 - \epsilon_3) - \langle v_2^2\rangle]\}/ \{[(\epsilon_1 - \epsilon_2)(\epsilon_1 - \epsilon_3)]^2 - 2(\epsilon_1 - \epsilon_2)(\epsilon_1 - \epsilon_3)\langle v_2^2\rangle + \langle v_2^4\rangle + [\tilde{\kappa}(\epsilon_1 - \epsilon_3)]^2\} \tag{35}$$

From standard Gaussian integrals, we obtain

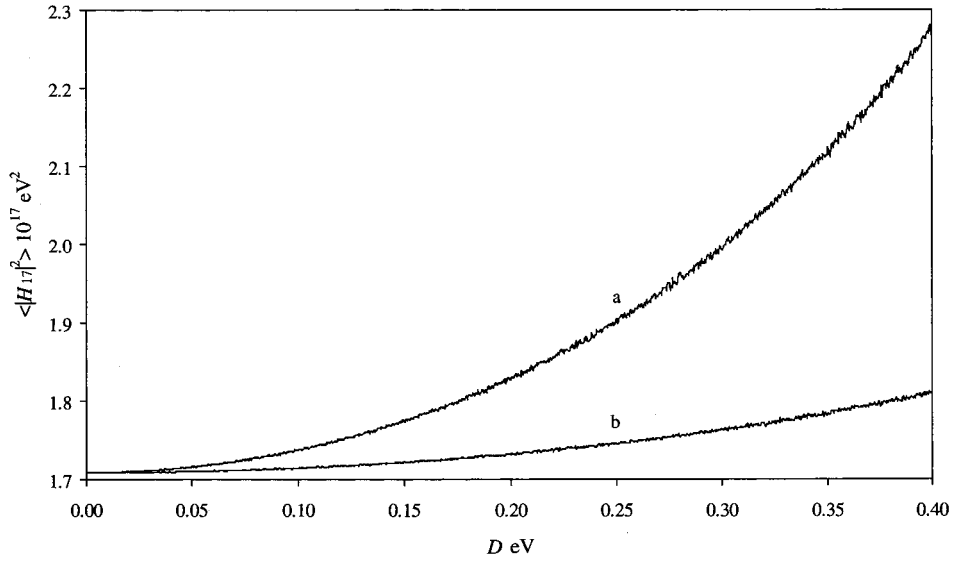

Figure 4. Variation of $\langle|H_{17}|^2\rangle$ with diagonal disorder (a) when disorder occurs at all bridge sites and (b) when disorder occurs at bridge 2.

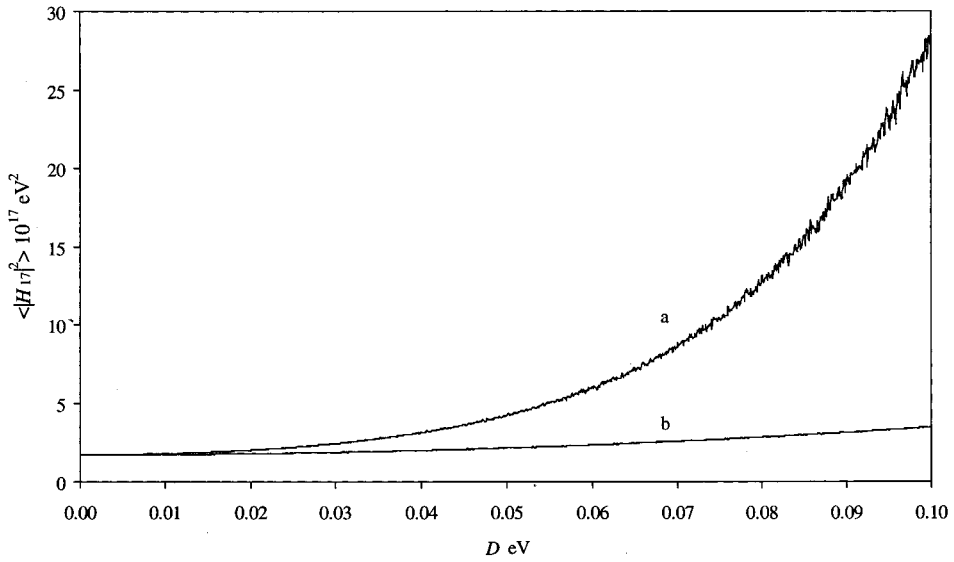

Figure 5. Variation of $\langle|H_{17}|^2\rangle$ with off-diagonal disorder (a) for all adjacent site interactions and (b) for interaction between bridge 2 and bridge 3.

$$\langle v_2^2\rangle = \mu^2 + D^2 \tag{36a}$$

$$\langle v_2^4\rangle = \mu^4 + 6\mu^2D^2 + 3D^4 \tag{36b}$$

where upon substituting into eq 35 gives the final analytical form for $\mathrm{Re}\langle t_1\rangle$. The graph of $\mathrm{Re}\langle t_1\rangle$ thus obtained using eqs 35 and 36 is given by the solid line in Figure 3b. The analytical form of $\mathrm{Re}\langle t_1\rangle$ agrees well with the Monte Carlo result and again shows the enhancement of the coupling attenuation factor when disorder is slowly increased.

By applying the Green's function method introduced in section 2, we demonstrate that diagonal (Figure 4) and off-diagonal (Figure 5) disorder can result in an increase in the effective superexchange coupling. This is easily rationalized from the constituent attenuation terms (t_i) of H_{17} which experience the same effects of disorder as discussed above. For a N-bridged system where eq 33 is applicable, the rate of change of the superexchange coupling with energy gap $(E - \epsilon - \Delta)$ is roughly proportional to $-N(E - \epsilon - \Delta)^{-(N+1)}$. When the excitation site energy ϵ_i is displaced by an equal amount either away from or closer to the tunneling energy, the resulting increase in the superexchange coupling from the latter is greater than the reduction caused by an increased in the energy band gap. This means that diagonal disorder effectively lowers the energy gap between the donor and the bridge sites, thus facilitating the superexchange mechanism. Similarly, the rate of change of the superexchange coupling with intersite interaction v is proportional to $Nv^{(N-1)}$ so that an enhanced effective energy transfer rate is also achieved with off-diagonal disorder. Another feature worth noting in Figures 4 and 5 is that the effects of fluctuations on all bridge energies or all interbridge couplings are more apparent than that on either single v_i or ϵ_i since an ensemble average of all t_i's are now needed to treat $\langle|H_{17}|^2\rangle$. A study on molecular wires reported by Ratner and co-workers[38a] revealed that electron conductance in molecular wires is affected in an analogous fashion by disorder. In particular, when the Fermi level lies outside the wire bandwidth, the superexchange conductance increases initially with energetic disorder before decaying away.

We now turn our attention to the effects of next-to-nearest-neighbor interaction and in particular on the relative contributions of pathway 1 (eq 10) and pathway 2 (eq 11) to the effective

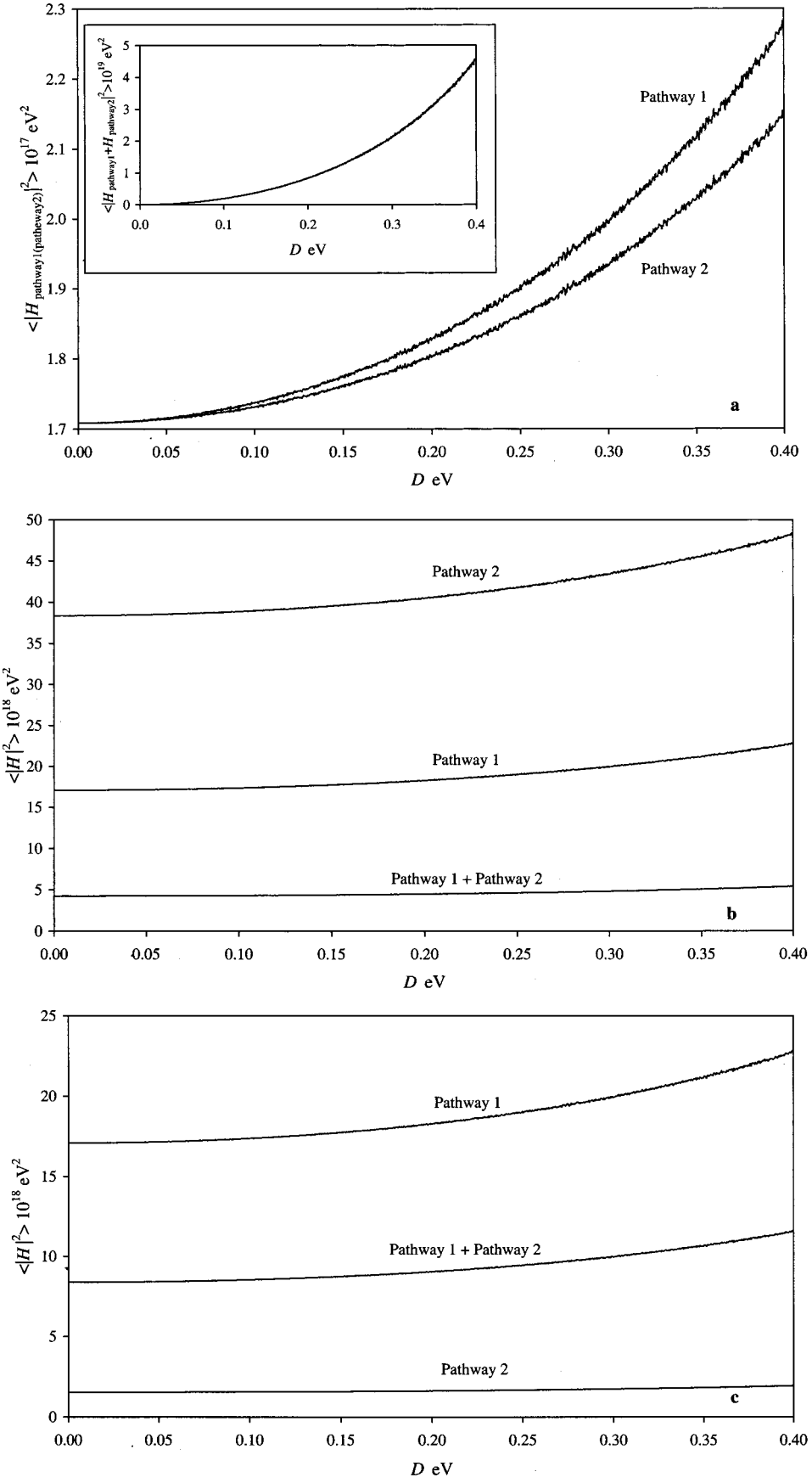

Figure 6. Effects of *diagonal* disorder on the contribution to the effective superexchange coupling of pathway 1 ($\langle|H_{17}^{\text{pathway1}}|^2\rangle$) and pathway 2 ($\langle|H_{17}^{\text{pathway2}}|^2\rangle$) along with their resultant contribution ($\langle|H_{17}^{\text{pathway1}} + H_{17}^{\text{pathway2}}|^2\rangle$) when (a) the next-to-nearest-neighbor interaction NNN = 0.003337 eV, (b) NNN = 0.005 eV, and (c) NNN = 0.001 eV.

superexchange coupling in the presence of disorder. Notice from the McConnell model, when the NNN and NN interactions are of the same sign, a destructive interference occurs between the two pathways. Figure 6a describes $\langle|H_{17}|^2\rangle$ as a function of

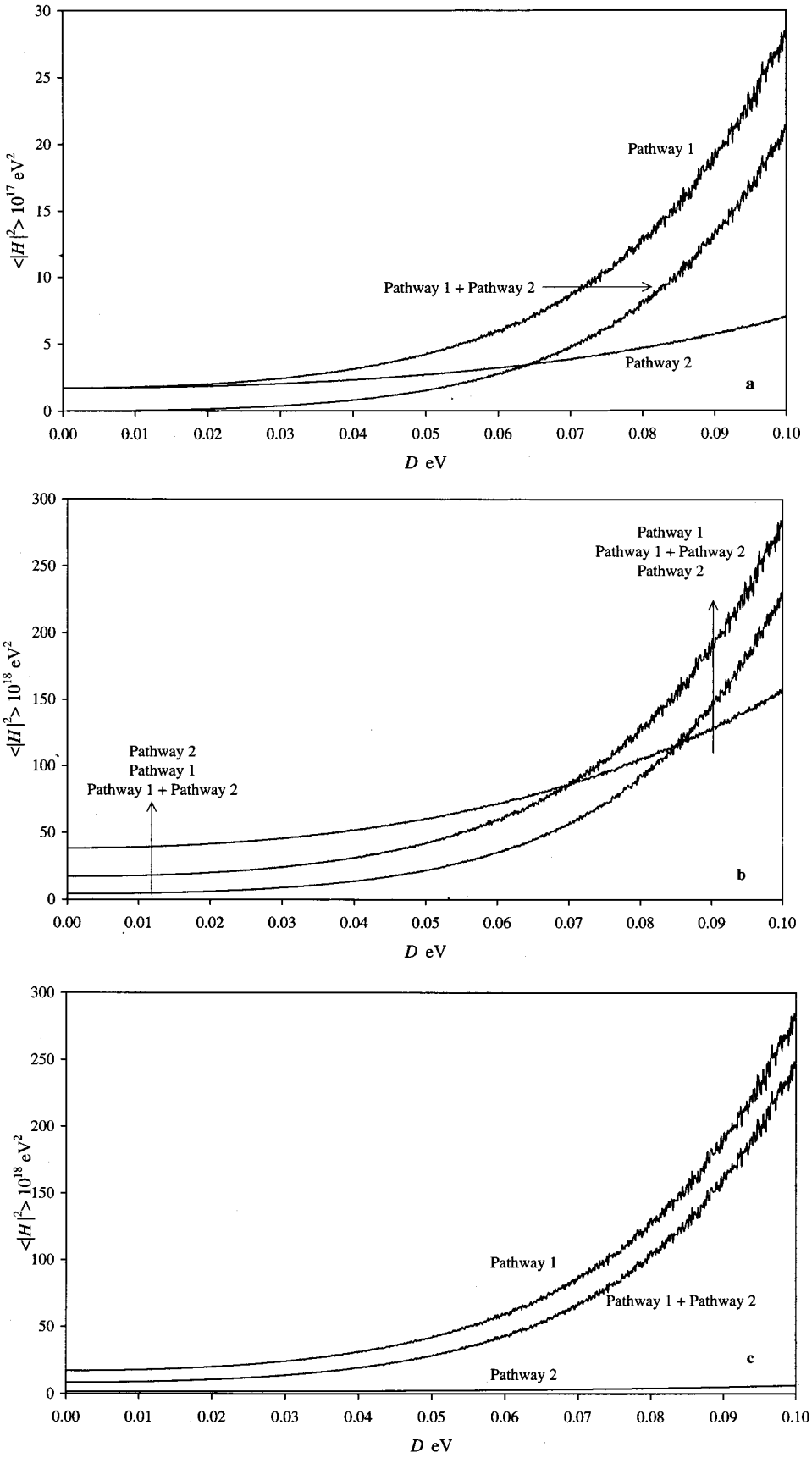

Figure 7. Effects of *off-diagonal* disorder between adjacent bridge coupling on the contribution to the effective superexchange coupling of pathway 1 ($\langle|H_{17}^{\text{pathway1}}|^2\rangle$) and pathway 2 ($\langle|H_{17}^{\text{pathway2}}|^2\rangle$) along with their resultant contribution ($\langle|H_{17}^{\text{pathway1}} + H_{17}^{\text{pathway2}}|^2\rangle$) when (a) the next-to-nearest-neighbor interaction NNN = 0.003337 eV, (b) NNN = 0.005 eV, and (c) NNN = 0.001 eV.

bridge energy disorder for the two pathways (i.e., H_{17}^{pathway1} and H_{17}^{pathway2}) and their resultant contribution to the superexchange coupling (i.e., $H_{17}^{\text{pathway1}} + H_{17}^{\text{pathway2}}$). In this case, the NN interaction is 0.1 eV while the NNN interaction between sites

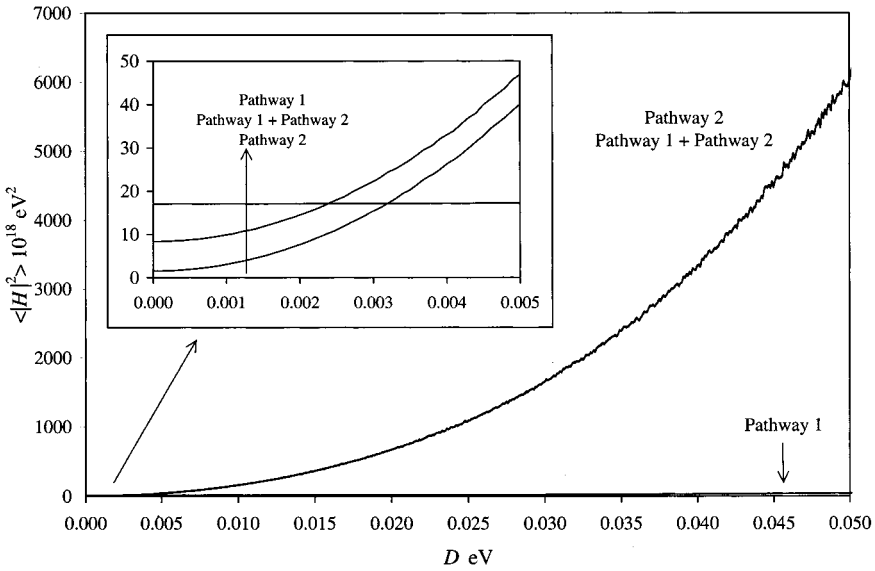

Figure 8. Effects of off-diagonal disorder between adjacent bridge coupling and non-nearest-neighbor interaction on the contribution to the effective superexchange coupling of pathway 1 ($\langle|H_{17}^{\text{pathway1}}|^2\rangle$) and pathway 2 ($\langle|H_{17}^{\text{pathway2}}|^2\rangle$) along with their resultant contribution ($\langle|H_{17}^{\text{pathway1}} + H_{17}^{\text{pathway2}}|^2\rangle$) when the next-to-nearest-neighbor interaction NNN = 0.001 eV.

2 and 4 in pathway 2 is 0.003337 eV. Both pathways are of equal importance in the absence of disorder which gives rise to a near-complete destructive interference and a diminished resultant contribution to the energy transfer rate. In this case, we name the NNN interaction as the optimum interaction. With the introduction of disorder, H_{17}^{pathway1}, H_{17}^{pathway2} and H_{17}^{pathway1} and $H_{17}^{\text{pathway1}} + H_{17}^{\text{pathway2}}$ increase in magnitude with the longer pathway 1 becoming the dominant route. We can assign $-(E - \epsilon - \Delta) = \zeta$ when the bridge sites are energetically far removed from the donor. From eqs 10 and 11, we get

$$\zeta_{D=0} = \frac{H_{23}H_{34}}{H_{24}} \tag{37}$$

for $D = 0$ eV. Pathway 1 is the primary factor in the resultant contribution when $(H_{17}^{\text{pathway1}} + H_{17}^{\text{pathway2}}) < 0$ is satisfied. For a disordered system, this condition can be translated into $\zeta_{D=0} > \zeta_D$ which is easily fulfilled since fluctuation of the site energies has been shown to reduce the energy band gap ζ_D.

As expected, when the NNN interaction is now increased to 0.005 eV, the shorter pathway 2 becomes the more important route taken by the excitation energy (Figure 6b) whereas when H_{24} is reduced to 0.001 eV, the longer pathway 1 prevails (Figure 6c) throughout all degrees of disorder. In general, when the next-to-nearest-neighbor interaction, H_{24}, is greater (smaller) than the optimum interaction, pathway 2 (pathway 1) is the dominant pathway.

Next we consider a system where fluctuation is centered on adjacent bridge couplings. The disorder-dependent behavior of the mean of the square of H_{17}^{pathway1}, H_{17}^{pathway2} and $H_{17}^{\text{pathway1}} + H_{17}^{\text{pathway2}}$ are presented in Figures 7a, 7b and 7c for NNN coupling = 0.003337, 0.005, and 0.001 eV respectively. Again an increase in $\langle|H_{17}|^2\rangle$ is observed when disorder sets in. Given the two possible nonexclusive pathways, we note that when H_{24} is either 0.003337 or 0.001 eV, the dominant energy tunneling path is pathway 1. This is also observed in the diagonal disordered system mentioned in the previous paragraph. An interesting feature is revealed when the next-to-nearest-neighbor interaction between bridges 2 and 4 is 0.005 eV (see Figure 7b). Even though the expected pathway 2 remains the principal pathway, its role in energy tunneling is reversed when the degree of disorder D is greater than 0.07 eV. At this region, the fluctuation is able to create a system where the NNN interaction becomes smaller than the optimum interaction brought about by an effective increase in the NN couplings. Pathway 1 therefore gains significance. When H_{24} is now allowed to undergo fluctuation, the shorter pathway 2 becomes the dominant route for all three cases of NNN interactions. We choose NNN coupling = 0.001 eV to illustrate this point. Figure 8 shows that pathway 1 is the dominant path at small degree of disorder but is negligible when $D > 0.0025$ eV. This is due to a relatively smaller optimum interaction formed when compared to the disordered NNN coupling. Note that an equal amount of NN disorder is unable to compensate for the decline in $|H_{17}^{\text{pathway1}}|$ relative to $|H_{17}^{\text{pathway2}}|$.

The above results emphasize the importance of disorder effects on the tunneling dynamics of excitation energy. The implications in this section are especially relevant for photochemists in pursuit of the ideal photomolecular device. Morrison et al.[40] have recently studied the kinetics of long-range through-bond energy transfer for a series of molecular photonic devices. More recently, we have reported[1a] the need to invoke the superexchange mechanism to fully explain the EET dynamics in a rigidly linked naphthalene dimer. Incorporation of high-energy gates and relays can help to facilitate or impede the rate of superexchange energy transfer. Therefore, by careful selection of these units, various pathways via the gates or relays will contribute differently to the superexchange coupling depending on disorder effects. One has the potential to control the rates of energy transfer in such systems.

(b) Nonorthogonal Basis. It is well-known that the rate of superexchange energy transfer k decreases exponentially with an increasing donor−acceptor separation R, such that

$$k \propto \exp(-\beta R) \tag{38}$$

where β is the effective decay constant per bond. In the first half of this section, we shall examine the effects of disorder on the attenuation factor β. To mimic a real molecular system, the bridge molecule used in our study was chosen to closely resemble ethene.[7b] Ab initio studies of the electronic factors responsible for excitation transfer within an ethene dimer have previously been performed.[7b] The average HOMO ionization

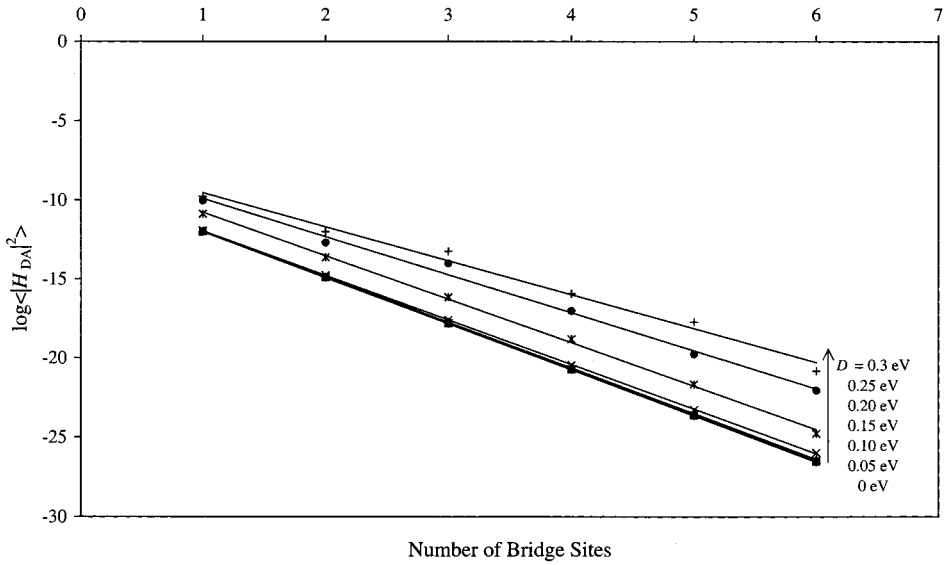

Figure 9. Bridge length dependence of $\log\langle|H_{17}|^2\rangle$ for different values of disorder. The gradients of the linear lines decrease with increasing disorder, indicating a weaker exponential falloff in a more disordered system.

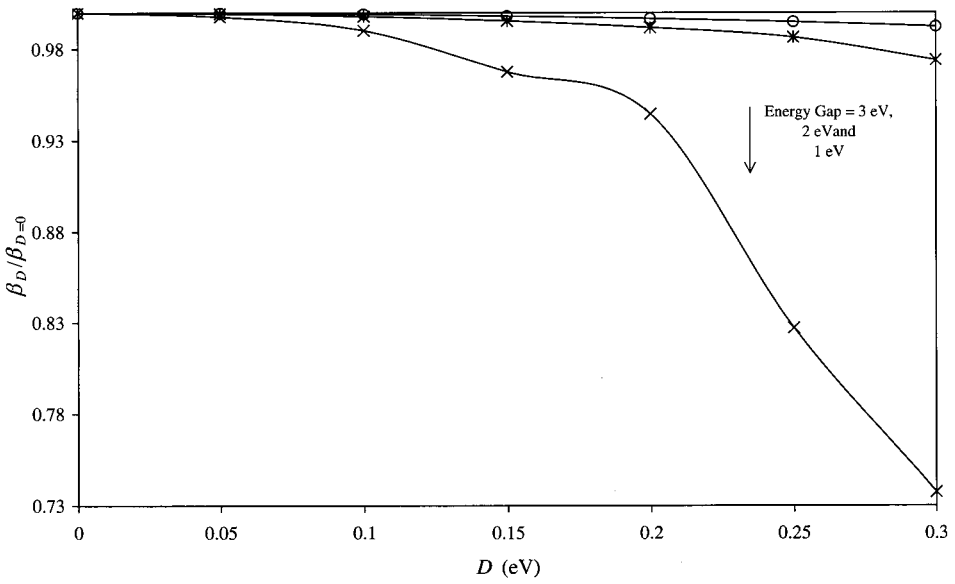

Figure 10. Plot of attenuation factor ratio $\beta_D/\beta_{D=0}$ as a function of disorder D.

potential of each bridge was set at 22 eV while the LUMO ionization potential ($I_{i'}$) was varied from 30 to 28 eV. This corresponded to an energy gap of 3 eV (24 195 cm^{-1}) to 1 eV (8065 cm^{-1}), respectively. The orbital overlap terms, s_{ab} and $s_{a'b'}$, and $\bar{A}$ required to compute the through-configuration interaction between adjacent chromophores are 0.01, 0.005, and 1 eV, respectively. The donor (acceptor)- bridge coupling is fixed at 0.001 eV.

The dependence of the superexchange transfer rate (i.e., $\langle|H_{DA}|^2\rangle$) on the bridge length is illustrated in Figure 9 for $I_{i'} = 28$ eV. A straight line is obtained irrespective of the amount of disorder operating in the system. This suggests that even at the maximum disorder ($D = 0.3$ eV), the energy is tunneling through a barrier at a rate that decreases exponentially with an increase in the separation distance between donor and acceptor (i.e., superexchange mechanism). The most striking feature observed is the weaker falloff of k with distance when the fluctuation is gradually increased. This is easily followed from the gradient, g, of the lines in Figure 9 since β is simply $-1.1515g$. The attenuation factor can be easily shown to be

$$\beta \approx -\ln(|v/\zeta|) \tag{39}$$

where v relates to adjacent bridge coupling. Since disorder effectively reduces (enhances) the magnitude of donor-bridge energy gap ζ (v), β would naturally decrease.

To investigate what happens when the donor−bridge energy gap is changed, we first define

$$\hat{\beta} = \frac{\beta_D}{\beta_{D=0}} \tag{40}$$

where β_D and $\beta_{D=0}$ are the decay constants for disorder D and $D = 0$ eV, respectively. Figure 10 shows $\hat{\beta}$ as a function of D for energy gaps of 1 eV ($I_{i'} = 28$ eV), 2 eV ($I_{i'} = 29$ eV), and 3 eV ($I_{i'} = 30$ eV). In general, β_D and hence $\hat{\beta}$ decrease with disorder with a more prominent change in $\hat{\beta}$ observed when the energy gap is reduced. This implies that when the bridge molecules are modestly removed from the donor, the rate of decay of the superexchange coupling with an increase in donor−acceptor distance is greatly impeded in the presence of disorder. The tunneling mechanism via chemical bridges is therefore still

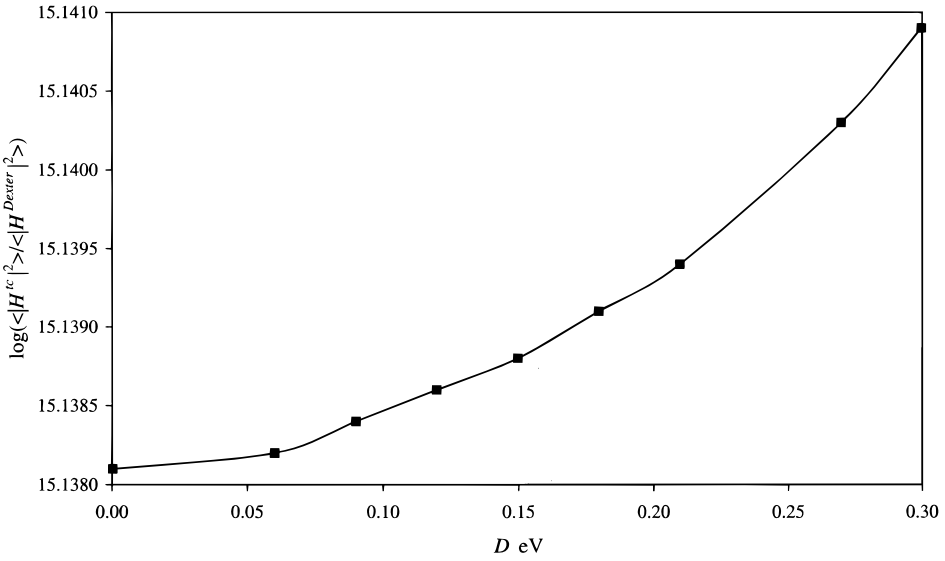

Figure 11. Plot of $\log\langle|H_{17}^{tc}|^2\rangle/\langle|H_{17}^{Dexter}|^2\rangle$ versus disorder D.

highly feasible in long disordered chains. We have recently shown[1a] that bath coupling with bridge molecules in systems with modest enough energy gap can activate a sequential energy transfer mechanism via the bridges. The competition between sequential and superexchange mechanisms would therefore take on a new dimension with the introduction of static disorder. Studies exploring the dual effects of bath fluctuation and static disorder on long-range energy transfer kinetics are underway.[41]

We conclude this section by comparing the superexchange coupling derived from through-configuration interaction (eq 19) and classical Dexter coupling (eq 18) between nearest bridge molecules. The calculated $|H_{17}^{Dexter}|$ and $|H_{17}^{tc}|$ when $I_{i'} = 30$ eV are 7.29×10^{-4} and 3.71×10^{-2} eV, respectively. Clearly, the through-configuration interaction is about 50 times larger than the Dexter interaction. By plotting $\log\langle|H_{17}^{tc}|^2\rangle/\langle|H_{17}^{Dexter}|^2\rangle)$ against disorder D in Figure 11, it is evident from the positive values obtained that the through-configuration interaction is the principal mode of "virtual" energy transfer throughout all degrees of disorder.

4. Conclusion

We have examined the effects of disorder on the superexchange coupling for several possible systems. An important conclusion is the remarkable enhancement of the effective donor−acceptor coupling when fluctuation is introduced into a disorder-free system. Molecular bridge arrays can be chemically designed with gate and relay units that allow next-to-nearest-neighbor interactions. The competing roles of individual pathways derived from the NNN interactions can be artificially manipulated by either changing the surrounding environment conditions (i.e., solvent polarity) or utilizing bridge molecules whose intermolecular couplings favor certain pathways. Experimentally, this means that one has the ability to control and optimize the rate of superexchange energy transfer. Our contribution in this paper should therefore provide some framework for the development of the optimized synthetic "light-harvesting" system.

Of great interest to us is the design of dendrimers as photon-harvesting arrays. We have recently shown[42] that electronic energy is efficiently transferred within a series of novel porphyrin funtionalized dendrimers with minimal loss during the energy migration process. Beratan et al.[43] have discussed some unique characteristics of the electronic communication between sites in these macromolecules. A well-designed dendrimer, in light of the "pathway control" model proposed here, can provide a critical study of the efficiency of energy funneling from the peripheral groups on the surface of the dendrimer to an interior energy trap.

We have also shown that the exponential falloff of the energy transfer rate with increasing donor−acceptor distance weakens when disorder is present. This may shed some light on the unprecedented ultrafast energy transfer observed in systems where the donor and acceptor are substantially separated (see the Introduction for the systems studied in this laboratory). Moreover, the impeded exponential decay of the superexchange coupling with distance is more apparent in a system where the bridge is only modestly removed from the donor. Finally, it is demonstrated that the superexchange coupling derived from through-configuration interaction is the dominant mode of superexchange energy transfer.

Acknowledgment. E.K.L.Y. thanks Dr. Richard Harcourt for valuable discussions on the subject of orbital-overlap dependent interaction. K.P.G. acknowledges the Australian Research Council for financial support of this work. The award of a Melbourne Research Scholarship to E.K.L.Y. is also acknowledged. The authors are grateful to the ORMOND High-Performance Computing facility for use of the Cray J916 computer.

References and Notes

(1) (a) Yeow, E. K. L.; Haines, D. J.; Ghiggino, K. P.; Paddon-Row, M. N. *J. Phys. Chem. A* **1999**, *103*, 6517. (b) Ghiggino, K. P.; Yeow, E. K. L.; Haines, D. J.; Scholes, G. D.; Smith, T. A. *J. Photochem. Photobiol. A: Chem.* **1996**, *102*, 81. (c) Scholes, G. D.; Ghiggino, K. P. *J. Chem. Phys.* **1995**, *103*, 8873.

(2) (a) Andrews, D. L.; Demidov, A. A. *Resonance Energy Transfer*; John Wiley and Sons: Chichester, UK, 1999. (b) Van der Meer, W. B.; Coker, G.; Chen, S. S.-Y. *Resonance Energy Transfer*; VCH Publisher: New York, 1994.

(3) Speiser, S. *Chem. Rev.* **1996**, *96*, 1953.

(4) *J. Phys. Chem. B* **1997**, *101*, 7197−7359. Papers presented at the Light-Harvesting Physics Workshop, Bristonas, Lithuania, 14−17 September 1996.

(5) Jordan, K. D.; Paddon-Row, M. N. *Chem. Rev.* **1992**, *92*, 395.

(6) McConnell, H. M. *J. Chem. Phys.* **1961**, *35*, 508.

(7) (a) Harcourt, R. D.; Scholes, G. D.; Ghiggino, K. P.*J. Chem. Phys.* **1994**, *101*, 10521. (b) Scholes, G. D.; Harcourt, R. D.; Ghiggino, K. P. *J. Chem. Phys.* **1995**, *102*, 9574. (c) Scholes, G. D.; Harcourt, R. D. *J. Chem. Phys.* **1996**, *104*, 5054.

(8) Evenson, J. W.; Karplus, M. *J. Chem. Phys.* **1992**, *96*, 5272.
(9) Goldman, C. *Phys. Rev. A* **1991,** *43*, 4500.
(10) Reimers, J. R.; Hush, N. S. *J. Photochem. Photobiol. A: Chem.* **1994**, *82*, 31.
(11) Cheong, A.; Roitberg, A. E.; Mujica, V.; Ratner, M. A. *J. Photochem. Photobiol. A: Chem.* **1994**, *82*, 81.
(12) (a) da Gama, A. A. S. *J. Theor. Biol.* **1990**, *142*, 251. (b) da Gama, A. A. S. *J. Mol. Struct. (THEOCHEM)* **1993**, *282*, 1.
(13) Malinsky, J.; Magarshak, Y. *J. Phys. Chem.* **1992**, *96*, 2849.
(14) (a) Onuchic, J. N.; de Andrade, P. C. P.; Beratan, D. N. *J. Chem. Phys.* **1991**, *95*, 1131. (b) Balabin, I. A.; Onuchic, J. N. *J. Phys. Chem.* **1996**, *100*, 11573.
(15) Fidder, H.; Knoester, J.; Wiersma, D. A. *J. Chem. Phys.* **1991**, *95*, 7880.
(16) (a) Stein, A. D.; Peterson, K. A.; Fayer, M. D. *Chem. Phys. Lett.* **1989**, *161*, 16. (b) Stein, A. D.; Peterson, K. A.; Fayer, M. D. *J. Chem. Phys.* **1990**, *92*, 5622. (c) Stein, A. D.; Fayer, M. D. *Chem Phys. Lett.* **1991**, *176*, 159.
(17) Potma, E. O.; Wiersma, D. A. *J. Chem. Phys.* **1998**, *108*, 4894.
(18) Hess, S.; Åkesson, E.; Cogdell, R. J.; Pullerits, T.; Sundström, V. *Biophys. J.* **1995**, *69*, 2211.
(19) Jimenez, R.; Dikshit, S. N.; Bradforth, S. E.; Fleming, G. R. *J. Phys. Chem.* **1996**, *100*, 6825.
(20) (a) Demchenko, A. P.; Sytnik, A. *J. Phys. Chem.* **1991,** *95*, 10518. (b) Demchenko, A. P. *Ultraviolet Spectroscopy of Proteins*; Springer-Verlag: Germany, 1986.
(21) Valeur, B.; Weber, G. *J. Chem. Phys.* **1978**, *69*, 2393.
(22) Gudowska-Nowak, E.; Papp, G.; Brickmann, J. *J. Phys. Chem. A* **1998**, *102*, 9554.
(23) Pande, V. S.; Onuchic, J. N. *Phys. Rev. Lett.* **1997**, *78*, 146.
(24) (a) Lopez-Castillo, J.-M.; Filali-Mouhim, A.; Plante, I. L.; Jay-Gerin, J.-P. *J. Phys. Chem.* **1995**, *99*, 6864. (b) Filali-Mouhim, A.; Lopez-Catillo, J.-M.; Plante, I. L.; Jay-Gerin, J.-P. *J. Phys. Chem.* **1996**, *100*, 12311.
(25) Lokan, N.; Paddon-Row, M. N.; Smith, T. A.; La Rosa, M.; Ghiggino, K. P.; Speiser, S. *J. Am. Chem. Soc.* **1999**, *121*, 2917.
(26) Ghiggino, K. P.; Smith, T. A. *Prog. React. Kinet.* **1993**, *18*, 375.
(27) Dexter, D. L. *J. Chem. Phys.* **1953**, *21*, 836.
(28) Mulliken, R. S. *J. Chim. Phys.* **1949**, *46*, 497, 675.
(29) Nishimoto, K.; Mataga, N. *Z. Phys. Chem.* **1957**, *12*, 335.
(30) Koopmans, T. *Physica* **1933**, *1*, 104.
(31) Wolfsberg, M.; Helmholz, L. *J. Chem. Phys.* **1952**, *20*, 837.
(32) Löwdin, P. O. *J. Mol. Spectrosc.* **1963**, *10*, 12.
(33) (a) Priyadarshy, S.; Skourtis, S. S.; Risser, S. M.; Beratan, D. N. *J. Chem. Phys.* **1996**, *104*, 9473. (b) Skourtiss, S. S.; Beratan, D. N. *Adv. Chem. Phys.* **1999**, *106*, 377.
(34) Hu, X. C.; Damjanovic, A.; Ritz, T.; Schulten, K. *Proc. Natl. Acad. Sci. U.S.A.* **1998**, *95*, 5935.
(35) Szabó, G. N.; Surján, P. R.; Ângyán, J. G. *Applied Quantum Chemistry*; D. Reidel Publishing Co.: Dordrecht, 1987.
(36) Rubinstein, R. Y. *Simulation and the Monte Carlo Method*; John Wiley & Sons: New York, 1981.
(37) (a) Lin, S. H.; Xiao, W. Z.; Dietz, W. *Phys. Rev.* **1993**, *47E*, 3698. (b) Liao, D. W.; Cheng, W. D.; Bigman, J.; Karni, Y.; Speiser, S.; Lin, S. H. *J. Chin. Chem. Soc.* **1995**, *42*, 177.
(38) (a) Kemp, M.; Mujica, V.; Ratner, M. A. *J. Chem. Phys.* **1994**, *101*, 5172. (b) Mujica, V.; Kemp, M.; Ratner, M. A. *J. Chem. Phys.* **1994**, *101*, 6856.
(39) Economou, E. N. *Green's Function in Quantum Physics*, 2nd ed.; Springer-Verlag: Berlin, 1983.
(40) Timberlake, L. D.; Morrison, H. *J. Am. Chem. Soc.* **1999**, *121*, 3618.
(41) Yeow, E. K. L.; Ghiggino, K. P., unpublished work.
(42) Yeow, E. K. L.; Ghiggino, K. P.; Reek, J. N. H.; Crossley, M. J.; Bosman, A. W.; Schenning, A. P. H.; Meijer, E. W. *J. Phys. Chem. B* **2000**, *104*, 2596.
(43) (a) Risser, S. M.; Beratan, D. N.; Onuchic, J. N. *J. Phys. Chem.* **1993**, *97*, 4523. (b) Onuchic, J. N.; Risser, S. M.; Skourtis, S. S.; Beratan, D. N. In *Molecular Electronics*; Jortner, J., Ratner, M., Eds.; Blackwell Science: Malden, MA, 1997.